

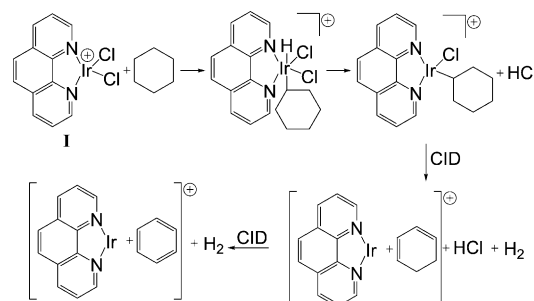
Intermolecular C–H Bond Activation by a Cationic Iridium(III) Dichloride Phenanthroline Complex**

Christopher A. Swift and Scott Gronert*

Abstract: It is demonstrated that a cationic iridium(III) dichloride phenanthroline complex is capable of C–H activation and H/D exchange. It can cleave benzylic and unactivated secondary C–H bonds, but exhibits unique selectivity when compared to similar systems that have been studied in the condensed phase. Gas-phase rate constants and kinetic isotope effects are reported for a variety of substrates and the analysis is supported by DFT calculations at the M06/QZVP level.

C–H activation has been described as the “holy grail of chemistry” and remains a very active research field.^[1–6] However, the ability to initiate reactivity at unactivated C–H bonds remains a challenge. In the past, cationic iridium(III) complexes have been shown to be effective catalysts for the activation of C–H bonds in the condensed phase and related chemistry has been demonstrated in the gas phase.^[7–14] Much of the previous work has utilized Cp* ligands on iridium with only a few examples of other ligand systems.^[9,12,15,16] Here we report the first example of bimolecular C–H activation by a cationic iridium(III) dichloride phenanthroline complex in the gas phase. This is a 14-electron species with a tetracoordinate iridium. The work includes kinetic measurements and is supported by computational modeling using density functional theory.

Using a modified ion-trap mass spectrometer,^[17] iridium(III) dichloride phenanthroline complex **I** was produced in the gas phase by electrospray ionization (ESI). While surveying its reactivity as a catalyst for diazoester decomposition, we were surprised by the observation of a relatively rapid reaction with the cyclohexane that was used to dilute the diazo ester. With cyclohexane, **I** mainly gives addition with the loss of HCl, which we interpret as a C–H activation process followed by reductive elimination of HCl (Scheme 1, Figure 1).^[10] This reactivity pattern follows what has been observed by the group of Bergman with other cationic iridium(III) systems.^[18] However, unactivated secondary C–H bonds are not cleaved in the condensed phase by cationic Ir^{III} complexes such as Cp*(PMe₃)IrMeOTf.^[18] This difference highlights the unusual reactivity of the phenanthroline complex. The kinetics of the reaction were measured and the



Scheme 1. Reaction of compound **I** with cyclohexane.

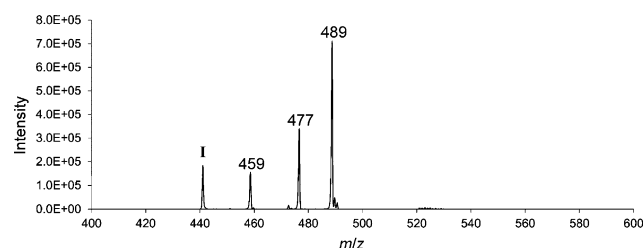


Figure 1. Mass spectrum of complex **I** reacting with cyclohexane. The reactant ion at m/z 441 is mainly the $^{191}\text{Ir}^{12}\text{C}_{12}^{14}\text{N}_2^1\text{H}_8^{35}\text{L}_2$ isotopomer. C–H activation corresponds to the peak at m/z 489, whereas the peaks at m/z 459 and 477 are single and double adducts of **I** with adventitious water in the ion trap.

Table 1: Rate constants for complex **I**.^[a]

Neutral Reagent	$k^{[a]}$	Efficiency ^[b]	Product ratio ^[c]
cyclohexane	0.7	9 %	100:0
toluene	4.9	59 %	95:5
[D ₈]toluene	4.3	52 %	46:54
ethylbenzene	6.4	82 %	100:0
isopropylbenzene	5.9	78 %	16:84

[a] Rate constants in units of $10^{-10} \text{ cm}^3 \text{ molecule}^{-1} \text{ sec}^{-1}$. [b] k/k_{coll} for which the collision rate is calculated by the method of Su and Bowers.^[20] [c] HCl loss/adduct.

process has an efficiency ($k_{\text{observed}}/k_{\text{collision}}$) of nearly 10 % (Table 1). Upon application of collision-induced dissociation (CID), we observe an additional loss of HCl and H₂, which we interpret as a dehydrogenation producing a cyclohexadiene complex (see Figure S1 in the Supporting Information, SI). When this complex is selected and CID is applied again, we then observe a loss of H₂, forming a benzene complex (Figure S2).

[*] C. A. Swift, Dr. S. Gronert
Department of Chemistry, Virginia Commonwealth University
1001 W. Main St., Richmond, VA 23284 (USA)
E-mail: sgronert@vcu.edu

[**] Support from the National Science Foundation (CHE-1300886) is acknowledged. We also thank the reviewers for very helpful comments.

Supporting information for this article is available on the WWW under <http://dx.doi.org/10.1002/anie.201500863>.

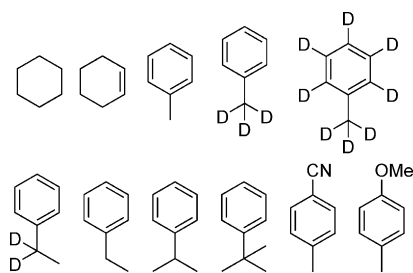
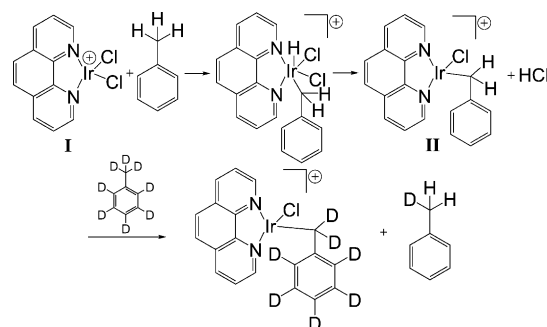


Figure 2. Neutral reagents that were allowed to react with complex I.

Inspired by the C–H activation and dehydrogenation reactions with cyclohexane, we turned to a wider set of species (Figure 2) to explore the generality of the C–H activation process and to establish reactivity patterns. Cyclohexene offers the ability to probe the dehydrogenation process that occurs with cyclohexane. Upon allowing complex **I** to react with cyclohexene, we observe a rapid loss of two HCl giving the cyclohexadiene complex without any application of CID (Figure S3). Further application of CID leads to a loss of H₂, producing the benzene complex (Figure S4).

Toluene provides an activated sp³ C–H bond as well as sp² C–H bonds. When complex **I** is allowed to react with toluene, rapid C–H activation is observed, as indicated by addition followed by the loss of HCl. To confirm the site of C–H activation, we employed [D₃]toluene. Although it is not possible to eliminate all interference from the multiple isotopes of Ir and Cl, it appears that reactions exclusively occur at the methyl group (Figure S6). Additionally, the reaction of **I** with benzene gives no C–H activation—only an adduct is formed. The preference for C–H activation at a benzylic group rather than on the benzene ring is in opposition to what has been reported in the condensed phase by Ito et al. with a similar cationic Ir^{III} bisoxazoline complex and by the group of Bergman with Cp*-ligated complexes.^[12,18] The group of Ito observed C–H activation at the *ortho*- and *para*-positions of the benzene ring rather than at the benzylic carbon. To probe for isotope effects, the kinetics were also measured with [D₈]toluene (Table 1). The primary kinetic deuterium isotope effect, k_H/k_D , is approximately 2.5 when comparing the partial rate constants for the formation of C–H activation products and suggests that the product-determining step is linked to a hydrogen transfer process. It appears that deuteration prevents the initial addition product from progressing through C–H activation to the products (see below) and therefore favors adduct formation.

To examine the potential for secondary reactions of the C–H activation products, we introduced a mixture of toluene and [D₈]toluene into the ion trap and allowed **I** to react with it. The initial toluene C–H activation product (**II**) was isolated in the ion trap using its mass selectivity capabilities (i.e., MSⁿ scanning) and then was allowed to react with the gas mixture. The reaction produces [D₇]-labeled **II**, indicating that **II** is also capable of C–H activation and can engage in a catalytic H/D exchange cycle (Scheme 2, Figure 3). The system reaches a pseudoequilibrium and the ratio of m/z 499 to 506 reflects the primary (as well as secondary) kinetic isotope effect in the process. Cationic iridium(III) complexes that are C–H



Scheme 2. H/D exchange process.

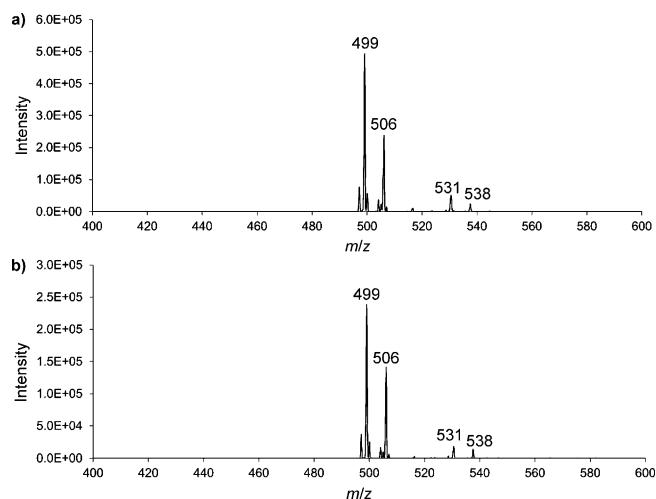


Figure 3. Mass spectra of complex **I** reacting with a 1:1 ratio of toluene:[D₈]toluene. The reactant ion at m/z 443 is mainly the most intense ¹⁹³Ir¹²C₁₂¹⁴N₂¹H₈³⁵Cl₂ isotopomer. The ion at m/z 499 corresponds to **II**. The ion at m/z 506 corresponds to **II**-d₇. The ions at m/z 531 and 538 are adducts of **II** and **II**-d₇ with adventitious MeOH, respectively. In (a), m/z 499 is isolated and allowed to react with the gas mixture. In (b), m/z 506 is isolated and allowed to react with the gas mixture.

activators in the condensed phase have also been shown to be low-temperature H/D exchange catalysts.^[19] The rate constant for the process is moderately low, $1.95 \times 10^{-11} \text{ cm}^3 \text{ molecule}^{-1} \text{ sec}^{-1}$, which corresponds to an efficiency of 2.5 %.

We next examined the impact of the substitution pattern on the C–H reactivity of benzylic systems. To do so, we allowed complex **I** to react with toluene, ethylbenzene, and isopropylbenzene. The rate constants (Table 1) are all near the collision-controlled limit, with ethylbenzene giving the highest rate constant. In isopropylbenzene, the product mixture shifts to mainly adduct formation. It is likely that steric effects with the tertiary center are inhibiting C–H activation (see below). To insure that these species were only giving activation at the benzylic center, experiments were also completed with [D₂]ethylbenzene. As expected, addition with exclusive loss of DCl is observed with this substrate. When *tert*-butylbenzene is allowed to react with **I**, no C–H activation is observed (an adduct is formed), indicating that unactivated primary centers are not suitable substrates.

To probe the effects of polar substituents on the C–H activation process, we allowed complex **I** to react with *p*-tolunitrile and 4-methylanisole. Ito et al. had reported that with bisoxazoline-ligated iridium(III) complexes, both electron-donating and electron-withdrawing groups increased the rate of C–H activation.^[12] With **I**, these substituted toluenes lead to stable adducts and it appears that they preferentially use their substituents to act as ligands for the iridium.

To gain more insight into the C–H activation process, the reaction of **I** with a secondary hydrogen in propane was modeled in Gaussian09^[21] using the M06 functional with an effective core potential (ECP) basis set on iridium (lanl2dz) and a 6-311 + G** basis set on the other atoms. The reported energies are from single-point calculations at the M06/QZVP level with thermal enthalpy corrections from the calculations with the mixed ECP/6-311 + G** basis set (test computations with the M06L functional gave similar results). Complex **I** has a roughly square planar coordination geometry, but the chlorines are tilted in and out of the plane leading to a C_2 -symmetric system with a C–N–Ir–Cl dihedral angle of 41° (Figure 4a). The initial reaction with propane leads to an

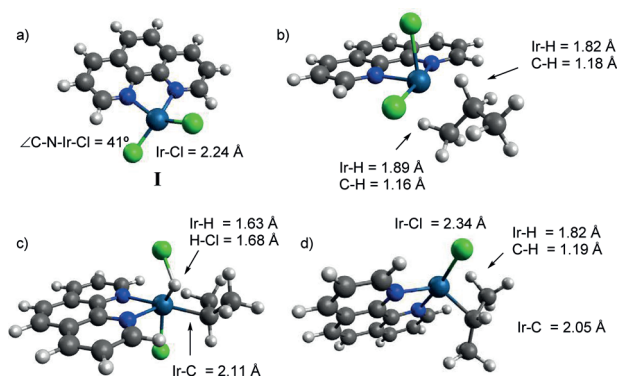


Figure 4. Geometries of key species in reaction of **I** with secondary hydrogen of propane. a) **I**; b) addition complex; c) transition state; d) product. Computations were completed with M06 functional and a mixed lanl2dz/6-311 + G** basis set.

unusually stable ion/molecule complex for a nonpolar substrate (enthalpy of association = -14.8 kcal mol⁻¹). The complex (Figure 4b) is pseudooctahedral at the iridium and is characterized by strong agostic interactions with a secondary (1.82 Å) and a primary hydrogen (1.89 Å). The C–H bonds are stretched to 1.18 and 1.16 Å, respectively. The strong agostic interactions between the iridium and hydrogen are consistent with calculations by Ziegler and co-workers, in which they described the delicate balance between agostic interactions and oxidative addition processes.^[22] We sought a pathway involving oxidative addition followed by reductive elimination of HCl. Although we were able to find a stable oxidative addition intermediate with the lanl2dz basis set on all atoms, it was less stable than the transition state leading to it when zero-point energies were included. Using the larger, mixed basis set we identified what appears to be a concerted (or nearly so) pathway with a transition state that is located late in the HCl expulsion pathway (Figure 4c). Intrinsic

reaction coordinate calculations link this transition state to the initial propane complex and an HCl complex of the reaction product (Figure S11). This transition state is 2.1 kcal mol⁻¹ below the separated reactants. Given the level of theory employed it is not possible to rule out a two-step mechanism with a distinct oxidative addition intermediate, but the calculations clearly suggest that the surface is relatively flat in this region. The computed barrier suggests a moderately fast reaction with secondary centers and is consistent with the experimental observations with cyclohexane. The HCl-expulsion product (Figure 4d) has an Ir–C bond (2.05 Å) as well as a strong agostic interaction with a methyl hydrogen (Ir–H = 1.82 Å). This structure is on the threshold of being an iridium hydride complex with a propene ligand. The overall process is calculated to be favorable by 14.8 kcal mol⁻¹.

A similar pathway was computed for the reaction with toluene (Figure S12). The C–H activation barrier is over 11 kcal mol⁻¹ below the entrance channel (the TS was linked to reactants/products by an IRC calculation). The reaction is computed to be exothermic by 8.3 kcal mol⁻¹. Using differences in computed enthalpy corrections (including zero-point energies), the calculations suggest a kinetic deuterium isotope effect of 4.0 at room temperature. Given the level of theory and possible dynamic effects related to the low barrier, this is an acceptable level of consistency with experiment. The initial complex is very stable (binding enthalpy of 26.9 kcal mol⁻¹) and this may explain the shift to adduct formation upon deuteration despite the low transition state energy. Computations also indicate that isopropylbenzene has a higher barrier than toluene in its reaction with **I** (Table S5, SI) and the transition state structure exhibits crowding between a chloride and methyl group. Computations on the reaction of **I** with benzene indicate that although the π interactions are comparable to those in toluene, the complex lacks the strong agostic interaction with a benzylic hydrogen. The transition state for C–H activation in benzene is 7.5 kcal mol⁻¹ below the reactants (3.5 kcal mol⁻¹ higher than that of toluene) and the process is exothermic by only 1.3 kcal mol⁻¹. The low exothermicity, reaction barrier, and the deep well for the reaction complex leads to a situation in which collisional cooling can efficiently lead to a stable adduct. In any case, it is clear that benzylic and allylic C–H bonds are kinetically favored over aryl C–H bonds because the iridium can engage in both π and agostic interactions.

In summary, a novel C–H activation system is described that can cleave unactivated secondary C–H bonds as well as benzylic C–H bonds. Computational modeling suggests a concerted pathway with low barriers. We are currently examining the reactivity of **I** and related species with a broader set of substrates.

Experimental Section

All experiments were conducted in a modified ThermoFinnigan LCQ Deca XP Plus quadrupole ion-trap mass spectrometer equipped with electrospray ionization (ESI). Iridium salts were dissolved in methanol at 10^{-4} – 10^{-5} M. Typical ESI conditions involved flow rates of 3–5 μ L min⁻¹ with needle potentials between 3.5 and 6 kV and heated capillary temperatures from 125 to 200°C. A notched wave-

form is used for isolating the iridium(III) species. Previous work indicates that the ion-trap environment is near room temperature.^[23] When a stable signal is obtained, neutral reagents can be spiked into the helium through a custom gas-handling system which has been previously described.^[17]

Kinetic measurements were completed by establishing an appropriate flow rate for the neutral reagent and varying the time between the isolation of the ion and the expulsion of all the ions to obtain a mass spectrum. Ten different time delays were used in each reaction. Reagent flows and time delays were varied to obtain plots that cover 2–3 half-lives of the ionic reagent. Data were obtained over at least 2 days with multiple neutral and ionic solution preparations. Kinetic plots showed sufficient linearity with correlation coefficients (r^2) of 0.98 or greater. A crude solution of the iridium(III) phenanthroline complex was generated by treating IrCl_3 with one equivalent of 1,10-phenanthroline in refluxing ethanol for 2 h followed by rotary evaporation. The resulting solid was resuspended in methanol and used without further purification. All neutral reagents were obtained from commercial sources in the highest purity available and used without further purification.

Keywords: C–H activation · gas phase · H/D exchange · iridium · isotope effects

How to cite: *Angew. Chem. Int. Ed.* **2015**, *54*, 6475–6478
Angew. Chem. **2015**, *127*, 6575–6578

- [1] B. A. Arndtsen, R. G. Bergman, T. A. Mobley, T. H. Peterson, *Acc. Chem. Res.* **1995**, *28*, 154–162.
- [2] R. G. Bergman, *Nature* **2007**, *446*, 391–393.
- [3] T. W. Lyons, M. S. Sanford, I. C. N. B. Formation, *Chem. Rev.* **2010**, *110*, 1147–1169.
- [4] D. Schröder, H. Schwarz, *Proc. Natl. Acad. Sci. USA* **2008**, *105*, 18114–18119.
- [5] J. Roithová, D. Schröder, *Chem. Rev.* **2010**, *110*, 1170–1211.
- [6] K. K. Irikura, J. L. Beauchamp, *J. Phys. Chem.* **1991**, *95*, 8344–8351.
- [7] S. R. Klei, K. L. Tan, J. T. Golden, C. M. Yung, R. K. Thalji, K. A. Ahrendt, J. A. Ellman, D. T. Tilley, R. G. Bergman, *Activation and Functionalization of C–H bonds*, American Chemical Society, Washington, DC, **2004**, pp. 46–55.
- [8] J. Lohrenz, H. Jacobsen, *Angew. Chem. Int. Ed. Engl.* **1996**, *35*, 1305–1307; *Angew. Chem.* **1996**, *108*, 1403–1405.
- [9] H. Suematsu, T. Katsuki, *J. Am. Chem. Soc.* **2009**, *131*, 14218–14219.
- [10] S. Niu, M. B. Hall, *J. Am. Chem. Soc.* **1998**, *120*, 6169–6170.
- [11] C. Hinderling, D. Feichtinger, D. A. Plattner, P. Chen, *J. Am. Chem. Soc.* **1997**, *119*, 10793–10804.
- [12] J. Ito, T. Kaneda, H. Nishiyama, *Organometallics* **2012**, *31*, 4442–4449.
- [13] J. M. Meredith, R. Robinson, K. I. Goldberg, W. Kaminsky, D. M. Heinekey, *Organometallics* **2012**, *31*, 1879–1887.
- [14] C. Hinderling, D. A. Plattner, P. Chen, *Angew. Chem. Int. Ed. Engl.* **1997**, *36*, 243–244; *Angew. Chem.* **1997**, *109*, 272–274.
- [15] C. Cheng, J. F. Hartwig, *J. Am. Chem. Soc.* **2015**, *137*, 592–595.
- [16] C. C. J. Seechurn, V. Sivakumar, D. Satoskar, T. J. Colacot, *Organometallics* **2014**, *33*, 3514–3522.
- [17] S. Netter, C. A. Swift, R. Joviliano, D. O. Noin, S. Gronert, *J. Am. Chem. Soc.* **2012**, *134*, 9303–9310.
- [18] S. R. Klei, J. T. Golden, P. Burger, R. G. Bergman, *J. Mol. Catal. A* **2002**, *189*, 79–94.
- [19] J. T. Golden, R. A. Andersen, R. G. Bergman, *J. Am. Chem. Soc.* **2001**, *123*, 5837–5838.
- [20] T. Su, M. T. Bowers, in *Gas Phase Ion Chemistry* (Ed.: M. T. Bowers), Academic Press, New York, **1979**, p. 83.
- [21] M. J. Frisch, G. W. Trucks, H. B. Schlegel, G. E. Scuseria, M. A. Robb, J. R. Cheeseman, G. Scalmani, V. Barone, B. Mennucci, G. A. Petersson, H. Nakatsuji, M. Caricato, X. Li, H. P. Hratchian, A. F. Izmaylov, J. Bloino, G. Zheng, J. L. Sonnenberg, M. Hada, M. Ehara, K. Toyota, R. Fukuda, J. Hasegawa, M. Ishida, T. Nakajima, Y. Honda, O. Kitao, T. Nakai, T. Vreven, J. A. Montgomery, Jr., J. E. Peralta, F. Ogliaro, M. Bearpark, J. J. Heyd, E. Brothers, K. N. Kudin, V. N. Staroverov, R. Kobayashi, J. Normand, K. Raghavachari, A. Rendell, J. C. Burant, S. S. Iyengar, J. Tomasi, M. Cossi, N. Rega, J. M. Millam, M. Klene, J. E. Knox, J. B. Cross, V. Bakken, C. Adamo, J. Jaramillo, R. Gomperts, R. E. Stratmann, O. Yazyev, A. J. Austin, R. Cammi, C. Pomelli, J. W. Ochterski, R. L. Martin, K. Morokuma, V. G. Zakrzewski, G. A. Voth, P. Salvador, J. J. Dannenberg, S. Dapprich, A. D. Daniels, Ö. Farkas, J. B. Foresman, J. V. Ortiz, J. Cioslowski, D. J. Fox, Gaussian09, Revision C.01 Gaussian Inc., Wallingford, CT, **2009**.
- [22] T. Ziegler, V. Tschinke, L. Fan, A. D. Becket, *J. Am. Chem. Soc.* **1989**, *111*, 9177–9185.
- [23] S. Gronert, *J. Am. Soc. Mass Spectrom.* **1998**, *9*, 845–848.

Received: January 29, 2015

Revised: March 9, 2015

Published online: April 13, 2015